ACS APPLIED MATERIALS & INTERFACES

RESEARCH ARTICLE

www.acsami.org

One-Step Production of Superhydrophobic Coatings on Flat Substrates via Atmospheric Rf Plasma Process Using Non-Fluorinated Hydrocarbons

Seul Hee Lee,[†,‡] Zachary R. Dilworth,[†] Erik Hsiao,[†] Anna L. Barnette,[†] Matthew Marino,[†] Jeong Hoon Kim,[§] Jung-Gu Kang,[§] Tae-Hwan Jung,[§] and Seong H. Kim*[,†]

[†]Department of Chemical Engineering, Pennsylvania State University, University Park, Pennsylvania 16803, United States

[§]SPS Co., Ltd. #305 Sinwoo Plaza, 83 Banwol-dong, Whasung-si, Gyunggi-Do, 445-330, South Korea

ABSTRACT: This paper describes the direct deposition of hydro carbon coatings with a static water contact angle higher than 150 using simple C6 hydrocarbons as a reactive gas in helium plasma generated in ambient air without any preroughening of the silicon (100) substrate. The film morphology and hydrophobicity are found to strongly depend on the structure of the reagent hydrocarbon. The films deposited with n-hexane and cyclohexane exhibited relatively smooth morphology and the water contact angle was only ~95°, similar to polypropylene. When benzene was used as a main reactive gas, the deposited film surface showed nanoscale textured morphology and superhydrophobicity with a water contact angle as high as 167°. Because the plasma is generated in air, all films show some degree of oxygen incorporation. These results imply that the incorporation of a small amount of oxygenated species in hydrocarbon films due to excitation of ambient air is not detrimental for superhydrophobicity, which allows the atmospheric rf plasma with the benzene precursor to produce rough surface topography needed for superhydrophobicity.

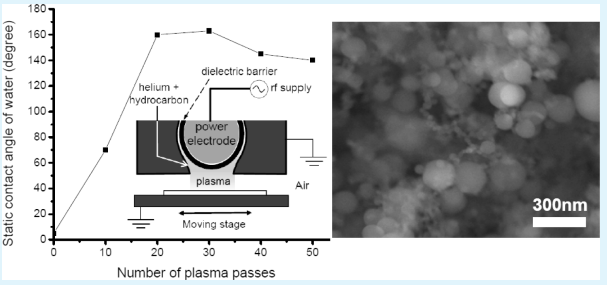

KEYWORDS: atmospheric plasma, superhydrophobic coating, benzene

INTRODUCTION

Superhydrophobicity has recently drawn a great deal of attention for both fundamental understandings and practical applications because of its potential applications in various technologies and consumer products such as weather-resistant or self-cleaning fabrics, windshields, display panels, microfluidic devices, etc.[1−5] Superhydrophobicity requires both right surface chemistry (mostly hydrophobic) and proper surface roughness.[5] Most superhydrophobic surface fabrication methods can be categorized into three strategies: (i) roughening hydrophobic materials, (ii) preparing surfaces with proper roughness and then depositing hydrophobic coatings, and (iii) depositing or growing coating layers with proper surface chemistry and structural features.[5] Plasma polymerization processes have widely been used for the second strategy because it can conformally deposit hydrophobic coatings on nano- and microstructured substrates to render the surface superhydrophobic properties.[6,7] By controlling the plasma conditions, the plasma deposition process can also be used for the third strategy, creating superhydrophobic films directly on flat substrates without preroughening of the substrates.[8−11] The latter process is more attractive in practical application point of view because it does not require any pretreatments of the substrate.

The plasma-based direct deposition of superhydrophobic coatings involves the formation of hydrophobic particulates in the plasma during the deposition process. Particulate formation is known to occur at relatively high density of reactive radicals and ions in the plasma.[12−14] Under these conditions, the diffusion path length of reactive species is very short and thus gas-phase reactions can readily take place. Upon reaching a critical number density, rapid condensation of the gas-phase species is triggered, and particulates are formed in the plasma.[15] Thus, the particulate formation in the gas phase and the production of textured rough film on a target substrate can be more readily achieved in atmospheric plasma condition than in low-pressure vacuum plasma generation conditions.

In previous plasma-based direct deposition studies, fluorinated hydrocarbons such as CF_4 were often used.[6,8,10,16] The primary reason is that the deposited films contain fluoride species which lowers the surface energy of the film. Another advantageous aspect of the fluorinated gases is that the C−F bond can easily be activated in the plasma, which makes it easy to achieve sufficiently high concentration of intermediate species to form particulates in the gas phase. One drawback, however, is that the fluorine radicals and ions generated during the plasma process are highly toxic and corrosive. Another issue is that the adhesion of fluorinated particulates to the substrate is weak.

Hydrocarbon precursor gases are more safe and benign for atmospheric plasma conditions. However, it was found that

Received: November 1, 2010
Accepted: January 11, 2011
Published: January 31, 2011

 © 2011 American Chemical Society

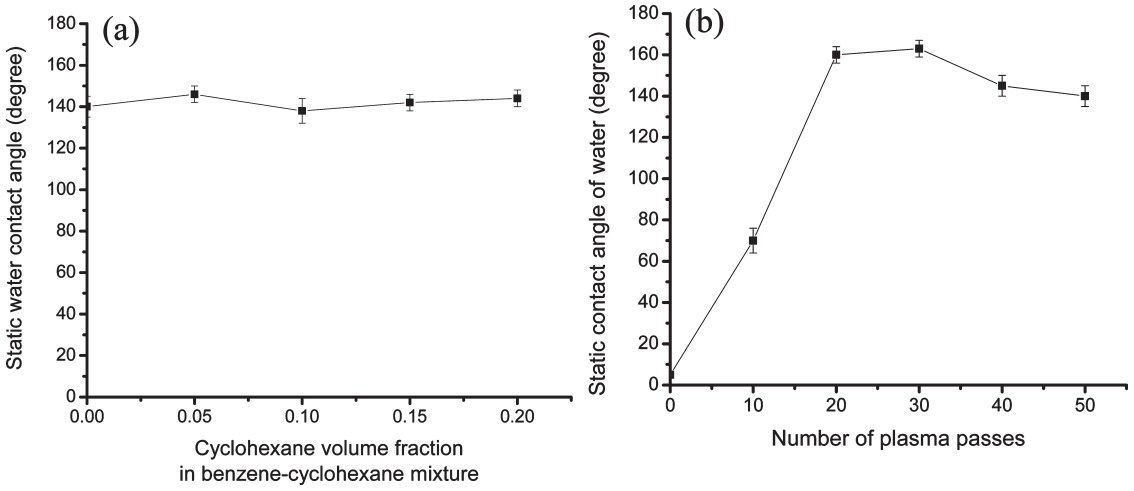

Figure 1. Static water contact angles versus (a) precursor composition at 50 passes and (b) number of passes at a fixed precursor mixture concentration (benzene:cyclohexane = 0.8:0.2) for the hydrocarbon films deposited with atmospheric rf. The total concentration of the precursor in the plasma process gas was 0.5% and the rf power was 150 W.

typical hydrocarbon precursor molecules such as methane and ethane cannot produce superhydrophobic coatings on smooth substrates. For example, the atmospheric CH_4/Ar plasma produces an extremely smooth polymer film on flat surfaces containing CH_2 backbones and CH_3 side groups.[7] In the CH_4/Ar plasma, the concentrations of reactive species (CH_2 and CH_3 radicals) are not high enough for condensation and formation of particulates in the gas phase. So, the reactive species diffuses to the substrate surface where polymerization reactions take place. When the substrate was textured with a proper roughness, then the hydrocarbon coating produced with the atmospheric CH_4/Ar plasma can provide a water contact angle higher than ~150°,[7] implying that the hydrocarbon-based film generated in the atmospheric plasma condition is sufficiently hydrophobic for an extremely high water contact angle as long as the proper roughness is provided.

This paper presents the one-step plasma deposition of superhydrophobic coatings using non-fluorinated hydrocarbon gases at ambient conditions. The plasma activation yield depends on the chain length and electronic structure of the precursor molecules.[17−20] Thus, it must be possible to use purely hydrocarbon sources with optimum chain lengths and electronic structures to increase the probability of particulate formation in the gas phase during the plasma activation process.[15,21] This will lead to production of a hydrocarbon film with rough surface morphology. C6 hydrocarbons with different structures—benzene (aromatic), n-hexane (linear aliphatic), and cyclohexane (cyclic aliphatic)—were tested. The film morphology and hydrophobicity vary with the structure of the reagent hydrocarbon. The films deposited with benzene consist of fine nanoparticles and show a static water contact angle as high as >160°. Although some oxygenated species are incorporated in the deposited film because the plasma is generated in air, this does not prevent the film from getting superhydrophobic water contact angles. When n-hexane and cyclohexane are used, the deposited films have a smooth surface morphology and exhibit a static water contact angle of 90−95°.

EXPERIMENTAL METHODS

The atmospheric radio-frequency (rf) glow-discharge plasma system was constructed with a custom-made plasma generator head and a 13.56 MHz rf supply with a LC matching unit. Details of the system were described previously.[7,8] Helium (99.99% purity) was used as a plasma gas and its flow rate was 4 L/min (lpm). A separate gas stream containing the precursor reagents was generated by flowing He through a bubbler containing n-hexane, cyclohexane, or benzene liquid. The plasma gas and precursor gas streams were combined in a mixing unit before entering the plasma head. The reagent gas stream flow rate was varied to obtain a certain concentration of precursor species (0.1−0.5 vol %) in the mixed gas stream. The rf power was controlled in the range of 100−200 W. The effective plasma area was ~1 cm wide and 10 cm long. Samples were mounted on a moving stage and repeatedly traveled back and forth across the glow-discharge plasma region at a speed of 1 cm/s. The distance from the plasma source and the sample was ~3 mm. Silicon (100) wafers were used as substrates.

The static water contact angle was determined with a homemade goniometer and calculating the slope of the tangent line of the drop at the liquid−solid−vapor interface line. The average contact angle was measured for water droplets with a volume of ~10 μL dropped and stayed on the film surface. The advancing and receding contact angles were measured with an automated goniometer (First Ten Angstrom Inc.) for representative samples showing the static contact angle larger than 150°. The surface morphology of the deposited film was analyzed with an optical microscope (Nikon, Optiphot 66) and a scanning electron microscopy (SEM; FEG-Nova 600 Nano SEM). Optical profilometry (Wyko NT1100) was used to estimate the surface roughness. Chemical analyses of the films produced with atmospheric rf plasma were performed with reflection-absorption infrared spectroscopy (RAIRS; Thermo Nicolet NEXUS 670) and X-ray photoelectron spectroscopy (XPS; VG Scientific/RHK Technology multi-chamber UHV surface science facility). The average thicknesses of the films deposited with n-hexane and cyclohexane were estimated with an ellipsometer (EllipsoTech, wavelength = 633 nm, angle = 70°).

RESULTS AND DISCUSSION

When benzene is used as a main precursor in the atmospheric plasma generated with He, the deposited film indeed produces a static water contact angle higher than 150°. Figure 1a plots typical water contact angles observed for the films deposited with benzene only and benzene-cyclohexane mixture precursors. The film deposited with benzene precursor only did not show a good stability and was easily removed by scouring with a water jet. When a small amount of cyclohexane was added to the process

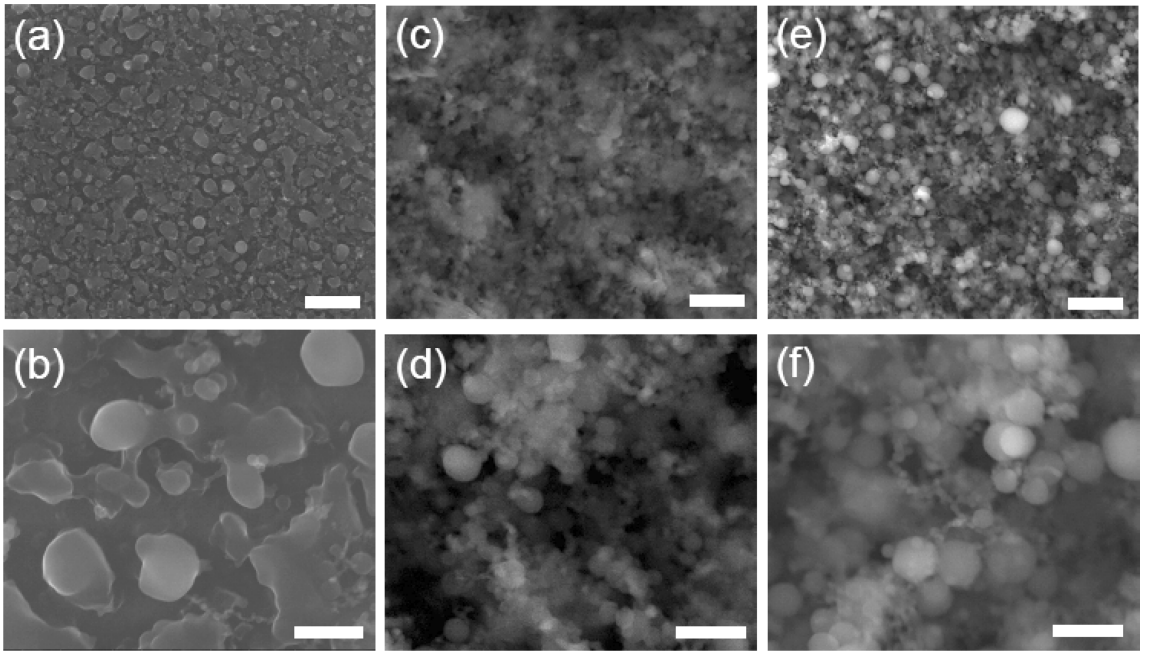

Figure 2. SEM images of the plasma-deposited films showing the static water contact angle of (a, b) 127, (c, d) 156, and (e, f) 167°. The films were deposited on a Si wafer with 150W atmospheric rf plasma using He gas containing 0.3 vol % benzene + cyclohexane (8:2) mixture. The scale bars in a, c, and e are 1 μm and those in b, d, and f are 300 nm. The SEM images were taken without metal conducting layer coating.

gas, more stable films were generated without deterioration of the water contact angle. Figure 1b shows the water contact angle of the film as a function of the plasma deposition times. When the films are produced by passing substrates under the benzene-cyclohexane plasma for ~30 passes, the static water contact angle was measured to be as high as ~160°. The advancing and receding contact angles measured for a set of samples were 157.0 ± 2.0 and 154.7 ± 1.4°, respectively. The roll-off angle of water droplets on these samples were less than 5° (typically ~3°). Upon further treatments, the water contact angle slightly decreases to ~145°.

The water immersion stability of the films deposited with the benzene-cyclohexane (8:2) mixed vapor was tested. There was no change in the static water contact angle measured after immersion in water for 10 min. This was a significant improvement compared to the superhydrophobic coating deposited with CF_4/H_2.[8] The films deposited with CF_4/H_2 were unstable and easily delaminated when water found pin hole defects or the edge of the film. This was due to the lack of strong bonding between the film and the substrate. In contrast, the film deposited with benzene/cyclohexane was not delaminated even if the entire film and substrate was immersed in water. It is believed that the homogenous coating of hydrocarbon layers formed with cyclohexane improves the adhesion between particulates formed from the benzene activation and the adhesion of particulates to the substrate.

The high water contact angle on the plasma-deposited films with the benzene-cyclohexane precursor can be explained with the film morphology. As the number of plasma passes increased, the sample surface lost its initial mirror-finish because of roughness of the deposited film. After 20 passes, the average and root-mean-square roughness of the deposited film increased to ~80 nm and ~120 nm, respectively. When the plasma pass was increased further, the optical profilometry failed to measure the surface roughness due to light scattering. Figure 2 shows the SEM images of three representative samples. The sample showing ~120° water contact angle is covered with particulates, but flat areas can still be seen between particulates. Upon further plasma cycles, more particulates are deposited and the substrate is fully covered, giving rise to a static water contact angle higher than 150°. The wide range of particle size distribution seems to be beneficial to increase the water contact angle to the superhydrophobic region.[22,23] Two distinct types of particulates are observed. One is round-shaped large particulates of 100−300 nm diameter. The other is irregularly aggregated 10−30 nm particulates. This bimodal distribution in particulate sizes implies that the density of reactive species inside the atmospheric rf plasma is high enough that coagulation and flocculation of particles take place in the gas phase.[24,25]

The chemical composition of the film was determined with XPS. Figure 3 presents XPS survey spectra of the hydrocarbon films deposited with the benzene-cyclohexane precursor gas. Although the precursor gas contains only carbon and hydrogen, the plasma-deposited films have oxygen and nitrogen. This is due to the activation of air in the atmospheric rf plasma. The C:N:O ratio was 85:3:12 in average. The C 1s high resolution spectra do not show discernable fine structures other than the broad main peak at 285 eV. A small asymmetric tail in the high binding energy side must be due to the oxygenated species. The weak shake-up peak of the benzene ring structure at ~293 eV is not observable. The O 1s peak is centered at ~533 eV, which can be attributed to aromatic C−O species.[26]

It is noteworthy that the film deposited at atmospheric pressure conditions contains oxygenated species, but it still gives the superhydrophobic water contact angle. The nitrogen, oxygen, and water molecules in the air are also activated in the plasma.[27] The highly energetic oxygen atoms and OH radicals can react with hydrocarbon fragments in the plasma.[28,29] Another possibility is the post-deposition oxidation of residual activated species such as radicals and dangling bond sites on the film surface upon exposure to air.[30] But, this post-deposition reaction fraction seems

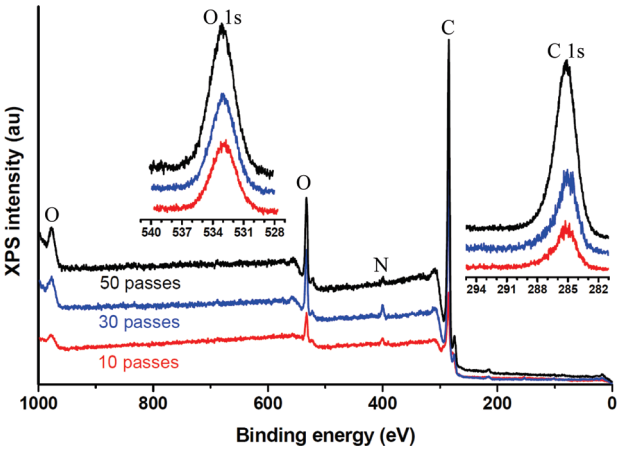

Figure 3. XPS survey spectra of the hydrocarbon films deposited with benzene-cyclohexane (8:2) precursor in the He plasma (precursor concentration = 0.3 vol %, plasma power = 150 W). The number of plasma treatment was 10, 30, and 50 passes. The insets are O 1s and C1s high-resolution spectra. The sample charging was compensated such that the C 1s main peak is positioned at 285 eV.

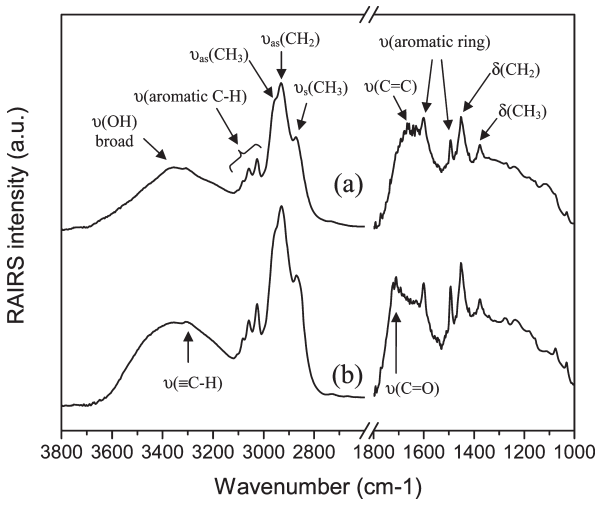

Figure 4. RAIRS spectra of the superhydrophobic coatings deposited using (a) pure benzene and (b) benzene-cyclohexane (8:2) mixture precursor gases. The total hydrocarbon concentration in the He plasma gas was 0.5% and the rf power was 150 W.

to be low. If the surface reaction was dominant, then the detected oxygenated species would mostly be present at the film surface. This would produce a fairly hydrophilic surface, which would give a low water contact angle. Similarly, the post-deposition incorporation of the oxygenated species is found to be small in low-pressure vacuum plasma deposition.[31] The fact that the water contact angle is higher than 150° implies that these oxygenated species are produced during the plasma deposition process and they are mostly locked inside the particulates composed of crosslinked hydrocarbon networks.

Figure 4 shows the RAIRS spectra of superhydrophobic films deposited using benzene and the mixture of benzene-cyclohexane (8:2) as a precursor in the atmospheric plasma. Although the aromatic structure cannot be detected in XPS, the characteristic vibration peaks of the aromatic ring structure are clearly observed in IR. These are the C−H stretch peaks of the phenyl ring in the 3082−3026 cm^{-1} region and the ring breathing modes at 1600 and 1492 cm^{-1}. These results imply that the aromatic ring structure of the precursor molecule is preserved to some degree in the deposited film.[32] In addition, large peaks of aliphatic CH_3 and CH_2 peaks are also detected at 2960, 2930, 2870, 1450, and 1377 cm^{-1}. There is a broad peak in the 1630−1680 cm^{-1} region corresponding to the C═C double bond vibrations and a weak peak at 3305 cm^{-1} which is assigned as the triple bonded ≡C−H stretch mode. These peaks indicate the fragmentation of the benzene structure and recombinative reactions of the fragments. Because the plasma is run in air, the hydroxyl peak is also observed as a broad peak centered at ∼3400 cm^{-1}.[32] When a small amount of cyclohexane is added (Figure 4b), then the carbonyl peak at 1720 cm^{-1} grows, which is negligible in the pure benzene precursor case. The presence of the hydroxyl and carbonyl groups might enhance particulate agglomeration in humid environment.[33]

The precursor molecular structure plays an important role in the deposition of the textured rough film for superhydrophobicity. The surface morphology of the films deposited with n-hexane and cyclohexane is not rough enough to provide the superhydrophobic water contact angle. An optical microscopy image of the film deposited with 0.3% cyclohexane is shown in the inset of Figure 5a, as an example. The water contact angle is measured to be only ∼95° regardless of the film thickness (Figure 5b) or the reagent gas structure (linear or cyclic alkane), as shown in Figure 5a. The contact angle measured for the films deposited with n-hexane and cyclohexane is very close to the one measured for polypropylene.[7]

As expected, the long chain alkane precursor gives a film deposition yield higher than the methane precursor. Figure 5b shows the film thickness as a function of hexane concentration in the atmospheric He plasma deposited by passing the substrates 10 times under the plasma at a speed of 1 cm/s. The He gas containing a concentration of 0.1 vol % of n-hexane and cyclohexane produces an average thickness for the deposited films of about 110 nm after 10 passes (∼11 nm per pass). When the reactive gas concentration is increased to 0.4%, the film thickness increases to ∼400 nm at the same number of passes (∼40 nm per pass). The difference between the n-hexane and cyclohexane cases appears to be insignificant. These deposition yields are much higher than the deposition yield of the CH_4/Ar plasma. The film growth with the CH_4/Ar plasma is about 6 nm per pass at a much lower scanning speed (0.1−0.2 cm/s), higher rf power (200−300 W), and higher methane concentration (0.5−1%).[7] The increased film deposition rate must be due to the enhanced plasma activation and decomposition rate of long chain alkanes.[17−19]

The chemical structures of the films deposited from n-hexane and cyclohexane were different from those deposited from benzene. Figure 6 presents the RAIRS data of the hydrophobic films deposited using n-hexane and cyclohexane precursors. The spectra of the hydrophobic films show well-defined aliphatic hydrocarbons and oxygen functionalities.[7] The peaks at 2962, 2930, 2870, 1450, and 1380 cm^{-1} correspond to the vibrations of asymmetric CH_3 stretching, asymmetric CH_2 stretching, symmetric CH_3 stretching, CH_2 deformation, and CH_3 deformation, respectively. The broad peak at 3450 cm^{-1} is due to the hydroxyl groups and the weak peaks at 1720 and 1610 cm^{-1} can be assigned to carbonyl groups (C═O). The peaks at 1105 and 1260 cm^{-1} can be ascribed to the C−O vibrations. These oxygenated species must be due to activation of air molecules inside the atmospheric plasma.

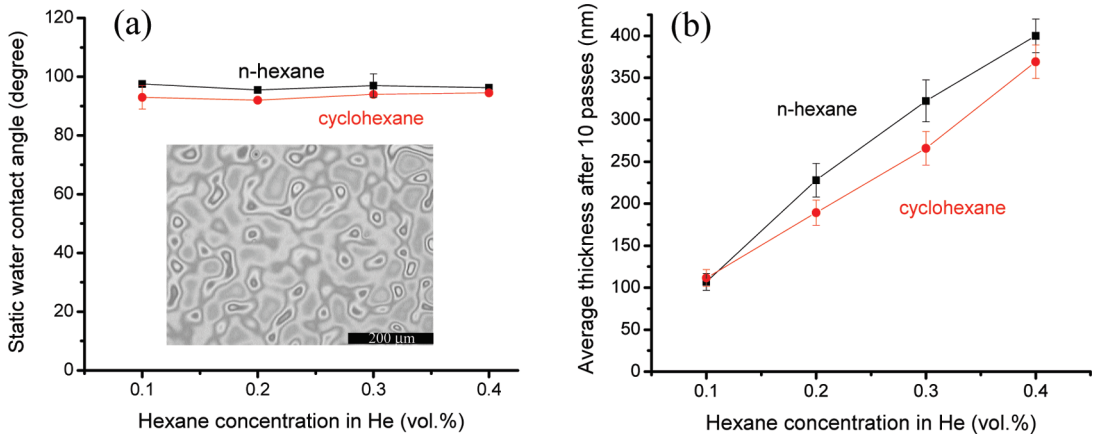

Figure 5. (a) Static water contact angle and (b) thickness of the deposited film as a function of the hexane concentration in the process gas. The film thickness was averaged over five different locations of each sample. The rf power was 150 W and the samples were passed 10 times under the plasma at a 1 cm/s speed. The inset in a shows an optical microscope image of the film deposited with 0.3% cyclohexane in the process gas.

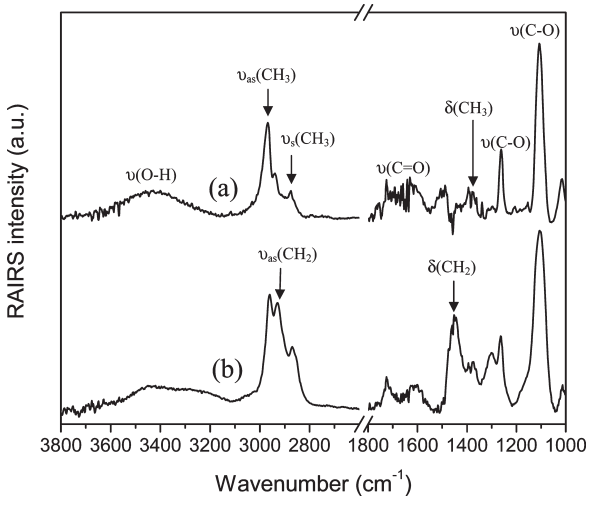

Figure 6. RAIRS spectra of the hydrocarbon films deposited with atmospheric rf plasma using (a) n-hexane and (b) cyclohexane as a precursor. The precursor concentration in the plasma process gas was 0.3% and the rf power was 150 W. The film was deposited by passing a substrate under the plasma 10 times at a 1 cm/s speed.

It is interesting to note that there are CH_3 groups observed for the film deposited with cyclohexane which contains only CH_2 units (Figure 6b). The CH_3 groups in the cyclohexane precursor film must be generated by recombination reactions of the cyclohexane fragments. Compared to the cyclohexane precursor film, the n-hexane precursor film does not have significant CH_2 vibration peaks (2930 and 1450 cm^{-1}). This would indicate high degree of C−C bond dissociation of n-hexane in the plasma. In contrast, the C−C bond in the cyclohexane structure seems to be preserved to a higher extent.

The mechanism for superhydrophobic coating formation from benzene-containing plasma must be due to the high activation cross-section of benzene in the plasma gas.[15,21] In the previous study, it was found that the CH_4/Ar plasma produces an extremely smooth polymer film on flat surfaces containing CH_2 backbones and CH_3 side groups.[7] In the CH_4/Ar plasma, the concentrations of reactive species (CH_2 and CH_3 radicals) are not high enough for condensation and formation of particulates in the gas phase. So, the reactive species diffuses to the substrate surface where polymerization reactions take place. The main gas-phase reactions are formation of C_2H_6, C_2H_2, and a small amount of C_2H_4 as well as CO.[34] As the chain length of the precursor molecule increases, the probability of plasma activation increases and so does the reactive species in the gas phase.[17−19] This explains the increased film deposition rate for n-hexane and cyclohexane precursors (Figure 5b). The fact that the films deposited from these C6 alkanes are smooth (Figure 5a) implies that the reactive radical concentration in the plasma is not high enough for solid particulate formation in the gas phase.[12−14] Or the gas phase condensation reactions do occur, but the reaction products do not form solid particulates. It is known that the plasma activation yield is much higher for aromatic hydrocarbons than aliphatic hydrocarbonds.[17,18] Condensation reactions of aromatic radicals can lead to large polycyclic aromatic compounds that can easily form solid particles in the gas phase.[32] These particles can further coagulate and flocculate into larger particles, resulting in the deposition of coatings with bimodal size distributions.[24,25]

CONCLUSIONS

It is commonly assumed that it is desirable to use oxygen-free and fluorine-containing process gases for deposition of superhydrophobic coatings in plasma deposition. This work demonstrates that the superhydrophobic coating deposition is possible without using fluorine-containing gases in plasma. When benzene is used as a reactive gas in atmospheric rf plasma, the condensation of reactive species in the plasma takes place to form particulates which are deposited on the substrate surface and exhibit superhydrophobicity although some oxygen species are incorporated into the film due to excitation of oxygen and water in air. Aliphatic hydrocarbon precursors cannot produce rough surface morphology needed to increase the water contact angle higher than 95°. These results suggest that the oxygen-free vacuum plasma is not necessary and the one-step superhydrophobic coating is possible with the plasma generated in ambient air using aromatic hydrocarbon precursors without preroughening or pretexturing of the substrate surface.

AUTHOR INFORMATION

Corresponding Author

*E-mail: shkim@engr.psu.edu.

Notes

[‡]Research intern from Yonsei University, Korea, through a Women In Engineering (WIE) program.

■ ACKNOWLEDGMENT

This research was supported by a grant from Construction Technology Innovation Program (CTIP) funded by the Ministry of Land, Transportation and Maritime Affairs (MLTM), Korea. The authors are grateful to Prof. M. K. Sunkara for kind support with SEM and XPS analyses. The authors acknowledge Prof. E. Volger for his help with advancing and receding contact angle measurements.

■ REFERENCES

(1) Nakajima, A.; Hashimoto, K.; Watanabe, T. *Monatsh. Chem.* **2001**, *132* (1), 31–41.
(2) Quere, D. *Rep. Prog. Phys.* **2005**, *68* (11), 2495–2532.
(3) Ma, M. L.; Hill, R. M. *Curr. Opin. Colloid Interface Sci.* **2006**, *11* (4), 193–202.
(4) Feng, X. J.; Jiang, L. *Adv. Mater.* **2006**, *18*, 3063–3078.
(5) Kim, S. H. *J. Adhes. Sci. Technol.* **2008**, *22* (3-4), 235–250.
(6) Lau, K. K. S.; Bico, J.; Teo, K. B. K.; Chhowalla, M.; Amaratunga, G. A. J.; Milne, W. I.; McKinley, G. H.; Gleason, K. K. *Nano Lett.* **2003**, *3* (12), 1701–1705.
(7) Kim, J. H.; Liu, G. M.; Kim, S. H. *J. Mater. Chem.* **2006**, *16* (10), 977–981.
(8) Kim, S. H.; Kim, J. H.; Kang, B. K.; Uhm, H. S. *Langmuir* **2005**, *21* (26), 12213–12217.
(9) Kim, S. H.; Kim, J. H.; Kang, B. K., . In *Nanoscience and Nanotechnology for Chemical and Biological Defense*; ACS Symposium Series; American Chemical Society: Washington, D.C., 2009; Vol. 1016, pp 323−336.
(10) Matsumoto, Y.; Ishida, M. *Sens. Actuators, A* **2000**, *83* (1-3), 179–185.
(11) Hozumi, A.; Takai, O. *Thin Solid Films* **1998**, *334* (1-2), 54–59.
(12) Mikikian, M.; Couedel, L.; Cavarroc, M.; Tessier, Y.; Boufendi, L. *Eur. Phys. J. Appl. Phys.* **2010**, *49*, 1.
(13) Teare, D. O. H.; Spanos, C. G.; Ridley, P.; Kinmond, E. J.; Roucoules, V.; Badyal, J. P. S.; Brewer, S. A.; Coulson, S.; Willis, C. *Chem. Mater.* **2002**, *14* (11), 4566–4571.
(14) Takahashi, K.; Tachibana, K. *J. Vac. Sci. Technol., A* **2001**, *19* (5), 2055–2060.
(15) Perrin, J.; Schmitt, J.; Hollenstein, C.; Howling, A.; Sansonnens, L. *Plasma Phys. Controlled Fusion* **2000**, *42*, B353–B363.
(16) Fresnais, J.; Chapel, J. P.; Poncin-Epaillard, F. *Surf. Coat. Technol.* **2006**, *200* (18-19), 5296–5305.
(17) Hirasawa, M.; Seto, T.; Kwon, S. B. *Jpn. J. Appl. Phys., Part 1* **2006**, *45* (3A), 1801–1804.
(18) Mok, Y. S.; Lee, H. W.; Hyun, Y. J.; Ham, S. W.; Nam, I. S. *Korean J. Chem. Eng.* **2001**, *18* (5), 711–718.
(19) Rosocha, L. A.; Kim, Y.; Anderson, G. K.; Lee, J. O.; Abbate, S. *IEEE Trans. Plasma Sci.* **2006**, *34* (6), 2526–2531.
(20) Ji, Y. Y.; Kim, S. S.; Kwon, O. P.; Lee, S. H. *Appl. Surf. Sci.* **2009**, *255* (8), 4575–4578.
(21) Foglein, K. A.; Babievskaya, I.; Szabo, P. T.; Szepvolygi, J. *Plasma Chem. Plasma Process.* **2003**, *23* (2), 233–243.
(22) Wier, K. A.; McCarthy, T. J. *Langmuir* **2006**, *22* (6), 2433–2436.
(23) Yao, X.; Chen, Q. W.; Xu, L.; Li, Q. K.; Song, Y. L.; Gao, X. F.; Quere, D.; Jiang, L. *Adv. Funct. Mater.* **2010**, *20* (4), 656–662.
(24) Watanabe, Y.; Shiratani, M. *Jpn. J. Appl. Phys., Part 1* **1993**, *32* (6B), 3074–3080.
(25) Courteille, C.; Hollenstein, C.; Dorier, J. L.; Gay, P.; Schwarzenbach, W.; Howling, A. A.; Bertran, E.; Viera, G.; Martins, R.; Macarico, A. *J. Appl. Phys.* **1996**, *80* (4), 2069–2078.
(26) Moulder, J. F.; Stickle, W. F.; Sobol, P. E.; Bomben, K. D. In *Handbook of X-ray Photoelectron Spectroscopy*; Physical Electronics, Inc.: Chanhassen, MN, 1995.
(27) Kim, S. H.; Kim, J. H.; Kang, B. K. *Langmuir* **2007**, *23* (15), 8074–8078.
(28) Dono, A.; Paradisi, C.; Scorrano, G. *Rapid Commun. Mass Spectrom.* **1997**, *11* (15), 1687–1694.
(29) Marotta, E.; Paradisi, C. *J. Am. Soc. Mass. Spectrom.* **2009**, *20* (4), 697–707.
(30) Jiang, H.; Grant, J. T.; Enlow, J.; Su, W. J.; Bunning, T. J. *J. Mater. Chem.* **2009**, *19* (15), 2234–2239.
(31) Choi, C. R.; Yeo, S. H.; Shon, H. K.; Kim, J. W.; Moon, D. W.; Jung, D. G.; Lee, T. G. *J. Vac. Sci. Technol., A* **2007**, *25* (4), 938–942.
(32) Shih, S. I.; Lin, T. C.; Shih, M. L. *J Hazard. Mater.* **2005**, *117* (2-3), 149–159.
(33) Mikhailov, E. F.; Vlasenko, S. S.; Podgorny, I. A.; Ramanathan, V.; Corrigan, C. E. *J. Geophys. Res. Atmos.* **2006**, *111* (D7), D07209.
(34) Kim, S. H.; Kim, J. H.; Kang, B. K. *J. Vac. Sci. Technol., A* **2008**, *26*, 123–127.